Integrating Reinforcement with 3D Concrete Printing: Experiments and Numerical Modelling

Jon Spangenberg[1(✉)], Wilson Ricardo Leal da Silva[2], Md Tusher Mollah[1], Raphaël Comminal[1], Thomas Juul Andersen[2], and Henrik Stang[3]

[1] Department of Mechanical Engineering, Technical University of Denmark, Kongens Lyngby, Denmark
josp@mek.dtu.dk
[2] Danish Technological Institute, Taastrup, Denmark
[3] Department of Civil Engineering, Technical University of Denmark, Kongens Lyngby, Denmark

Abstract. 3D Concrete Printing (3DCP) is a technology that recently has attracted the attention of both academia and industry. The technology offers an increased design flexibility and has been used at various scales, e.g. from furniture to bridges and houses. One of the current challenges in 3DCP is to produce load bearing structures in a single process, i.e. reinforced elements as part of 3DCP process. This is because the integration of vertical reinforcement during the printing process is not trivial. Although few reinforcement methods have been studied, a robust and efficient 3DCP reinforcement solution is yet to be coined. To support these studies in finding a reinforcement solution fit for 3DCP, while limiting experimental efforts, we offer a computational fluid dynamics (CFD) model that simulate concrete flow around rebars. The numerical model applies 1) an elasto-visco-plastic constitutive law to mimic the flow behavior of the concrete and 2) the volume of fluid method to track the free surface of the concrete. To validate the proposed model, 3DCP experiments are carried out by printing around horizontal and vertical rebars. The rheological behavior of the concrete is characterized on a rheometer using a vane-in-cup measuring system, and such data is included in the CFD model. The experimental and numerical results agree relatively well; providing a new venue for identifying printing strategies that ensures a good bonding between concrete and reinforcement.

Keywords: 3D concrete printing · Reinforcement · Computational fluid dynamics · Rheology

1 Introduction

Extrusion-based 3D Concrete Printing (3DCP) is a very promising digital construction technology that offers geometrical one-off structures in a time and cost-efficient manner. The 3DCP process is typically carried out by a gantry system or a robot arm, which guides a print head that deposits material along a toolpath to create a concrete structure in a layer-by-layer manner [1]. At present, one of the greatest challenges for

R. Buswell et al. (Eds.): DC 2022, RILEM Bookseries 37, pp. 379–384, 2022.
https://doi.org/10.1007/978-3-031-06116-5_56

this digital construction technology is to integrate printed layers and reinforcement. Therefore, researchers around the world have intensified their pursuit in finding robust methodologies to produce load-bearing 3DCP structures.

Examples of 3DCP reinforcement strategies that have been proposed include: a) penetrating reinforcing bars through printed layers [2] and b) the use of fiber reinforcement [3], to mention a couple. For a comprehensive review on 3DCP reinforcement strategies and classification thereof, refer to [4].

As in any research endeavor, the concepts described above require an extensive number of tests to be validated, yielding limitations to the number of reinforcement concepts that can be tested in practice. Therefore, numerical models have the potential to be a significant driver for 3DCP development [5] as they can reduce the experimental campaign necessary to explore a phenomenon as well as provide a mechanistic understanding of the process [6]. The latter was exemplified by Wolfs et al. [7], who used finite element method (FEM) simulations to investigate the early-age mechanical behavior of 3DCP. In addition, Computational Fluid Dynamics (CFD) models have been used to study the geometrical conformity of single- and multi-layer 3DCP deposition [8, 9].

These abovementioned models, however, have not been used to simulate the interactions between fresh printed layers and reinforcement rebars. To overcome that, this paper presents the first study where a CFD model is used to simulate 3DCP around horizontal and vertical rebars. The objective of the study is to investigate the CFD model's ability to predict the bonding behavior between concrete and reinforcement. The numerical simulations are compared to 3DCP experiments carried out with mortars.

2 Methodology

2.1 Materials and Experiment

The 3DCP around rebars was done with a cement-based mortar made of CEM I 52.5 R-SR 5 (EA), fine sand (<0.5 mm), limestone filler, admixtures, and water. The water: binder ratio was set at 0.39, and fine aggregates content accounts for 45% of the total dry mass. The admixtures dosage (by weight of cement) was set at 0.1% high-range policaboxilate-based water-reducing agent, a 0.5% polycarboxylic acid compound as retarder, and 0.1% viscosity-modifying agent based on a modified starch complex. The use of retarders enabled an open time of 2 h, i.e. the rheology of the mortar can be considered time-independent during the printing process (which took 15 min).

The mortar was prepared in an Eirich Intensive Mixer Type R08W. An Anton Paar rheometer MCR 502 was used to characterize the rheology of the mortar, which had a density of $\rho = 2100$ kg/m^3. Both the rotational and oscillatory tests were carried out using a vane-in-cup measuring device. The rotational rheometric tests, with a ramp-down controlled shear rate (CSR), determined the plastic viscosity $\eta_P = 7.5$ Pa and yield stress $\tau_Y = 630$ Pa.s. In addition, the oscillatory test showed that the unyielded mortar had a $G' = 200$ kPa within the linear viscoelastic (LVE) region. Thus, the mortar's rheology can be modelled with an elasto-visco-plastic (EVP) material behavior.

The 3DCP experimental setup is shown in Fig. 1. It included a 6-axis industrial robot with a custom-designed round nozzle and a progressive cavity pump equipped with a hopper and a long steel-wire rubber hose (refer to [8, 9] for details). The built platform

included a 25 mm thick plywood plate above which a rebar of diameter 8 mm was placed horizontally at the height of 14 mm rebar height from the base plate and held in place by vertical rebars. The setup was used to print a structure of four successive layers around the rebars. Details on the printing toolpath are illustrated in Fig. 2.

The extrusion Ø20 mm nozzle was placed at a height of 10 mm (nozzle height) above the built plate. For subsequent layers, the nozzle height was automatically increased by the 10 mm (i.e. the nominal height of a layer equals 10 mm). The extrusion speed was set at 0.91 dm^3/min and a nozzle travel speed was set at 35 mm/s. After the printed layers hardened, cross-sections were collected to analyze the interface between concrete and rebars. The cross-section for the rebar regions were obtained by slicing the printed element and scanning the cross-sectional area. To avoid damaging the printed samples during cutting, the samples were impregnated with epoxy resin in a vacuum chamber.

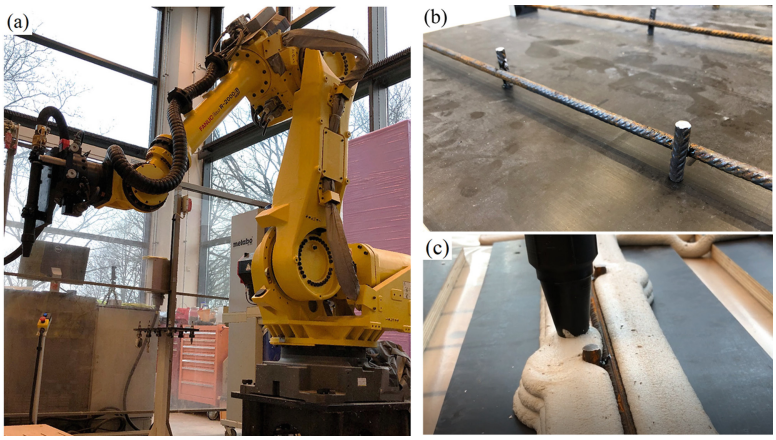

Fig. 1. 3DCP Experiment: (a) setup of 6-axis robot (Fanuc R-2000iC/165F) [8]; (b) built platform with placed rebars; (c) example of printing at the middle of third layer.

2.2 Computational Fluid Dynamics Model

The flow of the cementitious mortar was assumed incompressible and isothermal, and thus governed by the mass and momentum conservation equations. These were solved numerically using the commercial software FLOW-3D® v. 12.0. The software has previously been used for prediction of cementitious material flow, e.g. [10, 11]. The rheological behavior of the mortar was modelled as an EVP fluid, where the visco-plastic response followed a Bingham model with the plastic viscosity and yield stress that were determined experimentally as discussed in the previous section. The unyielded material was modelled with an elastic response that followed Hooke's law. The elastic shear modulus was set at 100 kPa, which is lower than the 200 kPa determined by rheological measurements. This reduction was applied to ease the numerical convergence, without substantially altering the numerical results. This assumption seemed reasonable since no substantial difference was found in the results when applying an elastic shear modulus

of 50 and 100 kPa. The equations that describe the EVP fluid can be found in [8], while the free surface of the mortar was modelled with the volume-of-fluid method.

To simulate the 3DCP experiments, two separate models were developed: deposition around the horizontal rebar (Model 1) and cross-shaped rebars (Model 2), cf. Figure 2. Both models include an extrusion nozzle, build plate, and computational domain (with size of 170 × 112 × 80 mm) in which the mortar was printed. The toolpath of the extrusion nozzle for the two models are also shown in Fig. 2. The top plane of the domain was an inlet boundary that holds an artificial solid component to prevent the flow outside the boundaries of the nozzle orifice. A no-slip boundary condition was imposed on the substrate and the domain was meshed with a Cartesian grid. The CFD model simulates four successive layers of length 125 mm around the horizontal rebar of length 50 mm and vertical rebar of height 40 mm (only for Model 2). The computational time of the simulations was around 18 days using 20 cores.

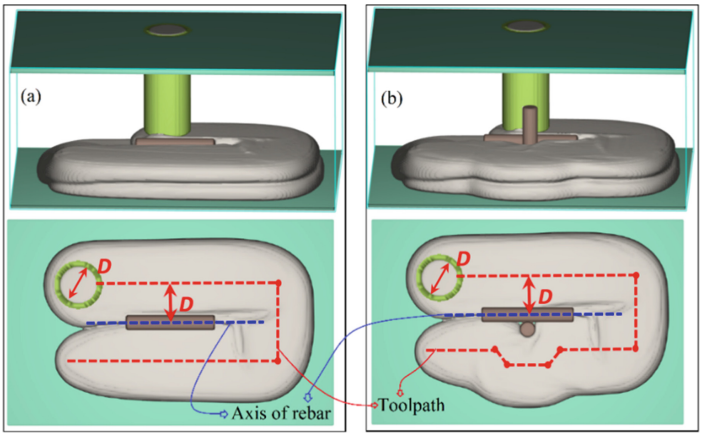

Fig. 2. Computational domain and toolpath. (a) Model 1: Deposition around horizontal rebar; (b) Model 2: Deposition around cross-shaped rebars.

3 Results and Discussions

The cross-sectional shape of the deposited layers around rebars in experiments and simulations are presented in Figs. 3a–d. The experimental results for the horizontal rebar in Fig. 3a illustrate that air voids are present both below and above the rebar as well as between layers 3 and 4. The latter is likely formed due to the deformation of previously printed layers, which increased the gap distance between the nozzle and layer 3, reducing the width of each independent strand in layer 4. A similar trend was observed in meso-structures produced with thermoplastic additive manufacturing [12]. The air voids around the horizontal rebar in Fig. 3a are smaller than the one between layers 3 and 4. This was attributed to the rebar occupying some of the space in between layer 2 and 3, which forced the mortar to be squeezed around the rebar. Another contributing

factor was the subsequent deformation of the layers when printing layer 4. In Fig. 3b, the mortar is printed around the cross-shaped rebars, in this scenario a greater number of air voids are observed. This is likely due to the vertical rebar restricting the mortar that was printed on either side of the reinforcement to merge. Especially, this scenario underlines the challenges related to integrating rebars with 3DCP.

Figure 3c, d presents the cross-sectional shapes of the simulations for both Model 1 and 2; showcasing that both models predict with high accuracy the location of air voids found in the printing experiments. The primary discrepancy between simulation and experiments was the width of the strands in the bottom layer (Fig. 3e, f). This might be attributed to slight differences in the rheological behavior and processing conditions (i.e. slight deviations between the distance of the nozzle to the rebars and base plate). Despite of that, the numerical results clearly illustrate the potential of the CFD model predictions. As such, the model can be exploited to find printing strategies that minimize or fully remove air voids in reinforced concrete structures produced with 3DCP.

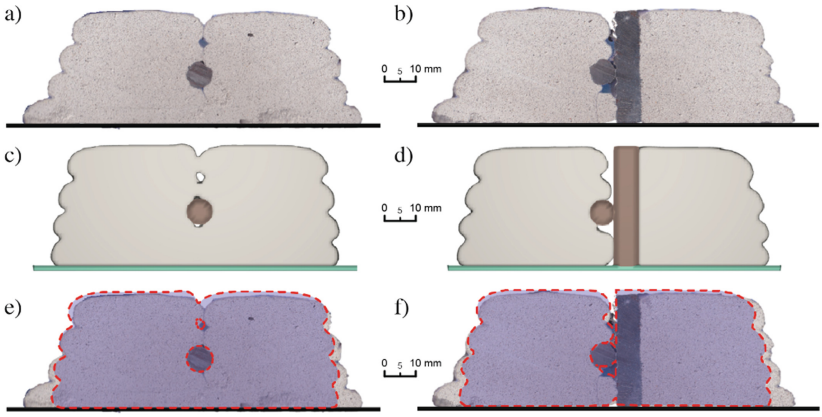

Fig. 3. Cross-sections of printed layers: (a, b) 3DCP experiment; (c, d) horizontal rebar (Model 1) and cross-shape rebars (Model 2); (e, f) overlay of simulation and printing results.

4 Conclusion

This paper presents experimental and numerical work on 3DCP around horizontal and vertical rebars. The printing results show that the printing strategy entrapped air voids both below and above the horizontal rebar as well as on the side of the vertical reinforcement. This highlights the non-trivial task of getting sufficient reinforcement encapsulation when applying 3DCP. A CFD model was developed to simulate the printing process, and a comparison between experimental and numerical results show that the model could predict the formation of voids around the rebars with great accuracy. Altogether, our research underlines the potential of using digital tools such as CFD modelling to digitally test and evaluate the outcome of printing strategies addressing reinforcement solutions for 3DCP applications.

Acknowledgement. The authors would like to acknowledge the support of the Innovation Fund Denmark (Grant no. 8055-00030B: Next Generation of 3D-printed Concrete Structures), the Danish Council for Independent Research (DFF) | Technology and Production Sciences (FTP) (Contract no. 8022-00042B), COWIfonden, and FLOW-3D® license support.

References

1. Buswell, R.A., Leal da Silva, W.R., Jones, S.Z., Dirrenberger, J.: 3D printing using concrete extrusion: a roadmap for research. Cem. Concr. Res. **112**, 37–49 (2018)
2. Marchment, T., Sanjayan, J.: Bond properties of reinforcing bar penetrations in 3D concrete printing. Autom. Constr. **120**, 103394 (2020)
3. Ding, T., Xiao, J., Zou, S., Yu, J.: Flexural properties of 3D printed fibre-reinforced concrete with recycled sand. Con. Build. Mat. **288**, 123077 (2021)
4. Mechtcherine, V., et al.: Integrating reinforcement in digital fabrication with concrete: a review and classification framework. Cem. Concr. Comp. **119**, 103964 (2021)
5. Roussel, N., Spangenberg, J., Wallevik, J., Wolfs, R.: Numerical simulations of concrete processing: from standard formative casting to additive manufacturing. Cem. Concr. Res **135**, 106075 (2020)
6. Mechtcherine, V., et al.: Extrusion-based additive manufacturing with cement-based materials – production steps, processes, and their underlying physics: a review. Cem. Concr. Res. **132**, 106037 (2020)
7. Wolfs, R.J.M., Bos, F.P., Salet, T.A.M.: Early age mechanical behaviour of 3D printed concrete: numerical modelling and experimental testing. Cem. Concr. Res **106**, 103–116 (2018)
8. Comminal, R., Leal, W.R., da Silva, T., Andersen, J., Stang, H., Spangenberg, J.: Modelling of 3D concrete printing based on computational fluid dynamics. Cem. Concr. Res. **138**, 106256 (2020)
9. Spangenberg, J., et al.: Numerical simulation of multi-layer 3D concrete printing. RILEM Tech. Lett. **6**, 119–123 (2021)
10. Spangenberg, J., et al.: Prediction of the impact of flow-induced inhomogeneities in self-compacting concrete (SCC). In: Khayat, K.H., Feys, D. (eds.) Design, Production and Placement of Self-Consolidating Concrete, pp. 209–215. Springer, Dordrecht (2010). https://doi.org/10.1007/978-90-481-9664-7_18
11. Jacobsen, S., Cepuritis, R., Peng, Y., Geiker, M.R., Spangenberg, J.: Visualizing and simulating flow conditions in concrete form filling using pigments. Con. Build. Mat **49**, 328–342 (2013)
12. Serdeczny, M.P., Comminal, R., Pedersen, D.B., Spangenberg, J.: Numerical prediction of the porosity of parts fabricated with fused deposition modeling. In: Proceedings of the 29th Annual International Solid Freeform Fabrication Symposium, Austin, TX, USA pp. 13–15 (2018)